



This is the accepted manuscript made available via CHORUS. The article has been published as:

Effect of high-temperature up-quenching on stabilizing offeutectic metallic glasses

Q. Cheng, P. F. Wang, H. Y. Jiang, L. Gu, J. Orava, Y. H. Sun, H. Y. Bai, and W. H. Wang Phys. Rev. B **103**, L100203 — Published 22 March 2021

DOI: 10.1103/PhysRevB.103.L100203

Letter

Effect of high-temperature up-quenching on stabilizing off-eutectic metallic glasses

Q. Cheng^{1,2}, P.F. Wang^{1,2}, H.Y. Jiang^{1,2}, L. Gu^{1,2}, J. Orava^{3,4*}, Y.H. Sun^{1,2,5*}, H.Y. Bai^{1,5,6}, W.H. Wang^{1,2,5}

- 1. Institute of Physics, Chinese Academy of Sciences, 100190, Beijing, China
- School of Physical Sciences, University of Chinese Academy of Sciences, Beijing, 100049,
 China
- 3. IFW Dresden, Institute for Complex Materials, Helmholtzstr. 20, 01069 Dresden, Germany
- Faculty of Environment, University of Jan Evangelista Purkyne in Usti nad Labem,
 Pasteurova 3632/15, Usti nad Labem 400 96, Czech Republic
- 5. Songshan Lake Materials Lab Dongguan, 523808, Guangdong, China
- Center of Materials Science and Optoelectronics Engineering, University of Chinese Academy of Sciences, 100049, Beijing, China

ABSTRACT

Fast heating calorimetry is used to study *in operando* the vitrification mechanism of off-eutectic Yb₄₇Mg₃₁Zn₁₉Cu₃ liquid at a cooling rate of 10,000 K s⁻¹. The glass forms only when it is quenched from between the melting and liquidus temperature, contradicting the need for full re-melting. Zinc-rich precipitates, forming on quenching from above the liquidus, deteriorate vitrification – that also offers an alternative explanation to what has often been considered as liquid-liquid transition. Application of an up-quenching thermal protocol facilitates the glass formation by removing the precipitates *in situ*; it is generally applicable and may extend the glass-forming range of other off-eutectic glasses. This research demonstrates a new strategy to develop bulk metallic glasses.

TEXT

Metallic glasses (MGs) are often formed at or near the deepest eutectic compositions upon cooling the liquid. $^{1-4}$ The glass-forming ability (GFA) of eutectic MGs is associated with the maximum reduced-glass-transition temperature ($T_{\rm rg}$) among all compositions, 3,5 where $T_{\rm rg} = T_{\rm g}/T_{\rm m}$ ($T_{\rm g} = T_{\rm g}/T_{\rm m}$) among all compositions, 3,5 where $T_{\rm rg} = T_{\rm g}/T_{\rm m}$ ($T_{\rm g} = T_{\rm g}/T_{\rm m}$) among all compositions or malized to the liquidus temperature ($T_{\rm l}$). The maximum at eutectic compositions because $T_{\rm m}$ is the lowest, and the reduced supercooling ($1-T_{\rm rg}$) required to make the glass is the largest. GFA of eutectic alloys is also connected to a solubility extension and 8 during rapid quenching. When phase separation is suppressed in rapid quenching, a liquid/solid multi-phase region in phase diagram diminishes, and a $T_{\rm 0}$ -line shows separating a liquid from a homogeneous solid solution. $T_{\rm 0}$ defines freezing (on cooling) of the liquid and $T_{\rm m}$ (on heating) of the solution, and refers to a temperature at which a liquid and a congruent crystalline phase equal in free energy. Near eutectic compositions, $T_{\rm 0}$ is low, the liquid is relatively stable, and glasses form more easily. The glass-forming composition can roughly be defined by a temperature region in which $T_{\rm g} > T_{\rm 0}$. Many other GFA criteria have been proposed. $T_{\rm 0} = T_{\rm 0} = T_{\rm$

Although many MGs are formed at or near eutectic compositions, the best GFA occurs at off-eutectic compositions as reported in many series of MGs. $^{5,12\text{-}16}$ For example, the best binary glass-former Cu_{64.5}Zr_{35.5} (at.%) MG (a critical rod diameter of 2 mm) is quenched from the side of its eutectic composition Cu_{61.8}Zr_{38.2} (bulk MG – BMG – cannot be casted) having steep liquidus line. 5 Good GFA of off-eutectic MGs is interpreted by the suppression of nucleation, crystal growth, and diffusion of the constituent elements. 9 According to the eutectic-coupled-zone theory, 12 the supercooling range that leads to the entirely eutectic growth, where the glass can be made during rapid quenching, is skewed towards the faceted phase owing to its persistence of growth difficulty. On the other hand, metastable-eutectic theory, used to explain solid-state amorphization, 17 is also applied to explain the off-eutectic GFA during rapid quenching. 14 Metastable eutectic compositions, off-eutectic in equilibrium phase diagram, are drawn in non-equilibrium phase diagram where a metastable eutectic region is tied by the extrapolation of two distant equilibrium liquidus lines. 14 Because $T_{\rm g}$ is

higher than the metastable eutectic temperature, off-eutectic MGs are capable to form in a such range when a primary intermetallic phase is suppressed. ^{14,17}

Recently, MG molten liquid relaxation has attracted great attention. Volumetric and viscosity hysteresis $^{18-19}$ or non-Arrhenius temperature-dependent viscosity 20 were detected near T_1 by electrostatic levitation. For $T > T_1$, $^{21-23}$ an abrupt shift in the position of the first peak of the structural factor was observed in synchrotron X-ray scattering on heating, $^{21-23}$ and a Knight-shift of Al in La₅₀Al₃₅Ni₁₅ melt was detected by nuclear magnetic resonance. 24 Using differential scanning calorimetry (DSC), some endothermic or exothermic events of unknown origin, additional to the main melting or crystallization peak, were recorded on heating or cooling, respectively. $^{21,25-26}$ These results were typically explained by polymorphic structural changes, including liquid-liquid transitions (LLTs), $^{18,21,23-28}$ or by non-cooperative to cooperative flow transitions. 20,29 In contrast, the possibility of compositional changes has rarely been mentioned. Here, precipitation is evidenced offering an alternative explanation to LLT.

For off-eutectic compositions, the multi-component liquid can enter multi-phase region at $T > T_{\rm m}$ on cooling from $T_{\rm l}$, giving high-risk precipitation that may deteriorate GFA. The success of making off-eutectic BMGs $^{5,12-16}$ suggests that phase separation, as a result of nucleating phases, can be suppressed. The questions are whether chemical diffusion or solute segregation are suppressed, too, and if not, whether GFA is affected by chemical diffusion or solute segregation. The answers shall be provided in this letter by using fast DSC (FDSC).

Metallic glass Yb₄₇Mg₃₁Zn₁₉Cu₃ was selected for the research because its thermal properties are easily accessible via FDSC. The gray line in **Fig. 1a** shows a representative FDSC of Yb₄₇Mg₃₁Zn₁₉Cu₃ MG on heating at $\phi_h = 2,000 \text{ K s}^{-1}$. Prior to heating, the glass was *in situ* cooled at $\phi_c = 10,000 \text{ K s}^{-1}$ from a quenching temperature $T_q = 693 \text{ K}$, i.e., 80 K above T_m (the gray line in **Fig. 1b**). The 693 K-cooled glass' calorimetry trace showed endothermic $T_g = 442\pm2 \text{ K}$, an exothermic crystallization marked by its onset $T_x = 503\pm5 \text{ K}$, and 1st-endo and 2nd-endo endothermic events. The former onset $T_m = 612\pm3 \text{ K}$ represents the melting of deepest-eutectic crystals, and the 2nd-endo represents melting of other crystalline phases, such as precipitates, with a peak temperature of 675 K. ^{31–32} Precipitation may occur either on

heating or on cooling resulting in compositional changes and eutectic crystallization of the residual supercooled liquid. For the 693 K-cooled glass, precipitation is likely to happen on heating because no exothermic signals were detected on cooling (the gray line in **Fig. 1b**).

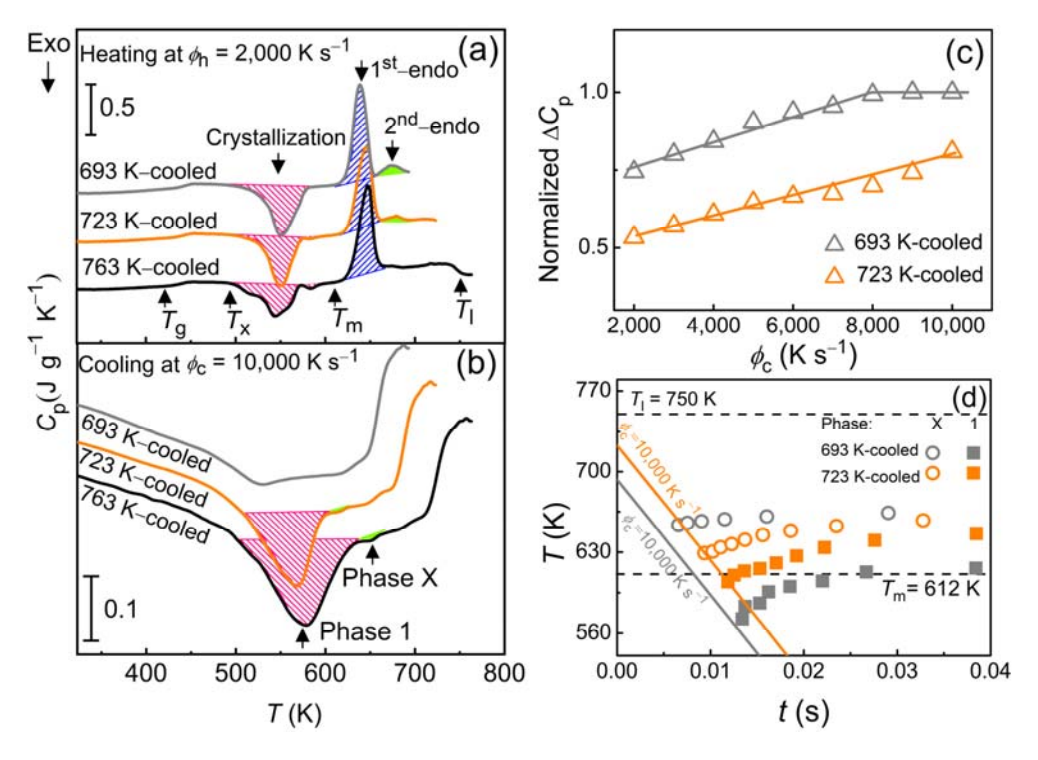


FIG. 1. Fast calorimetry traces of the off-eutectic Yb₄₇Mg₃₁Zn₁₉Cu₃ metallic glass (a) on re-heating and (b) on cooling. Part a: Re-heating traces of glasses quenched from 693 K (693 K-cooled), 723 K (723 K-cooled) and 763 K (763 K-cooled) measured at a heating rate (ϕ_h) of 2,000 K s⁻¹. The corresponding T_g , T_x , T_m and T_1 denote the characteristic temperatures of the glass transition, crystallization onset, melting and liquidus, respectively. The crystallization, the 1st endothermic (melting) and the 2nd endothermic (precipitation) peaks are colored in red, blue and green, respectively. Part b: Cooling traces measured at a cooling rate (ϕ_t) of 10,000 K s⁻¹. The high-temperature peak, colored in green, is termed as Phase X, and the low-temperature peak, colored in red, is termed as Phase 1. In both parts, offset to FDSC traces is applied for clarity. (c) The normalized change of specific heat at the glass transition (ΔC_p) is plotted vs ϕ_t . The normalization is made by dividing the ΔC_p of 10,000 K s⁻¹. (d) A measured continuous-cooling-transformation (CCT) diagram. No crystals are formed when the sample is quenched from 693 K, whereas Phase X and Phase 1 form when the liquid is

quenched from 723 K. The gray and the orange lines denote the cooling protocols of the 693 K- and 723 K-cooled glasses at constant $\phi_c = 10,000 \text{ K s}^{-1}$.

The orange and black lines in **Fig. 1a** & **b** represent heating and cooling traces of the same glass measured at the same rates but cooled from different T_q of 723 K and 763 K. For the 723 K-cooled glass, T_g , T_x , 1^{st} -endo and 2^{nd} -endo were all observed on heating with some qualitative differences to the 693 K-cooled glass. The 1^{st} -endo peak temperature (blue shading) increased, and the 2^{nd} -endo peak area (green shading) decreased in comparison with the 693 K-cooled glass. Those trends were more pronounced for heating the 763 K-cooled glass, where the 2^{nd} -endo peak nearly vanished. Also, multiple exothermic events, displayed as an individual peak and shoulders of the main exothermic crystallization peak, were observed on heating the 763 K-cooled glass. There were also stark differences on cooling. For both the 723 K- and 763 K-cooled glasses, two exothermic events were detected: a small exothermic peak (the green area) was detected at higher temperature, peaking at \sim 650 K, and a large exothermic peak (red shading) was observed at lower temperature. The former peak likely represents precipitates formed on cooling, labelled as $Phase\ X$, which serve as heterogeneous nucleation sites for the possible eutectic crystallization of $Phase\ I$, the main crystallization product.

There is a possibility that the 693 K-cooled glass was not fully glassy even if no exothermic peaks were detected on the cooling curves (**Fig. 1b**), e.g., some remaining crystals might not be melted at 693 K before cooling started. The intensity of the glass transition manifested as the change of specific heat from glass to supercooled liquid (ΔC_p) is plotted vs ϕ_c in **Fig. 1c**. For the 693 K-cooled glass, ΔC_p increased with the increasing ϕ_c until 8,000 K s⁻¹ and then remained constant; In contrast, ΔC_p of the 723 K-cooled glass continuously increased with the increasing ϕ_c . Because the increasing ΔC_p is a sign of semi-crystalline glass and the constant ΔC_p reflects self-doped or chemically homogeneous glass ³³, it is concluded that the 693 K-cooled glass is fully glassy.

A possible link between Phase X and Phase 1 was further studied on cooling from T_q of 693 K and 723 K at various ϕ_c . The onset-formation temperatures of Phase X and Phase 1 are collected as a continuous-cooling-transformation (CCT) diagram in **Fig. 1d**. For cooling at

10,000 K s⁻¹, Phase X and Phase 1 were not observed when cooled from 693 K, but both phases appeared when cooled from 723 K, demonstrating a strong T_q -dependence. For a given ϕ_c , the onset-temperature difference between Phase X and Phase 1 is larger for the 693 K-cooled than for the 723 K-cooled glass, suggesting that the formation of Phase 1 in the 693 K-cooled glass may be less influenced by Phase X. Because Phase 1 and Phase X are linked to eutectic crystallization and the precipitation on cooling respectively, the CCT diagram demonstrates that it may be easier to avoid both precipitation and crystallization on cooling from 693 K than from higher $T_q = 723$ K.

If two crystalline phases are formed in a sequence, then the first crystalline phase can act as the nucleation site for the second one. This is the case of cooling from 723 K and 763 K (**Fig. 1b**), where the Phase 1 growth (the first crystalline phase) is restricted by Phase X. ³⁴ If two crystalline phases formed simultaneously, as in the case of heating, then only one exothermic peak (the exo in **Fig. 1a**) may be detected as for the 693 K-cooled glass. Phase X is more stable when formed on heating rather than on cooling, signified by higher $T_{\rm m}$ and larger latent heat. Meanwhile, Phase 1 formed on cooling and heating also shows different shape of the 1st-endo peak, whose shape may partially shade the 2nd-endo event. Therefore, instead of being evidence of liquid transition, ²¹ the stability of Phase X may provide another explanation for the (non)- existence of the 2nd-endo event.

The fact that precipitates are easily formed at higher T_q may contradict the conventional understanding of GFA as one would expect the molten liquid to be homogeneous and free of un-melted nuclei at high T_q . In the present study, the selected T_q is lower than T_1 . In **Fig. 1a**, $T_1 = 750\pm3$ K is read as the end temperature of the deflection from the baseline of the 763 K-cooled glass. ³⁵ In a phase diagram, T_1 marks the transition temperature between a liquid and another multi-phase region, so below T_1 , chemical diffusion or solute segregation can take place before the onset of phase separation. One consequence of solute segregation is solute clustering as in the case of high-angle grain boundaries. ³⁶ Heating up higher $T > T_q$, yet below T_1 , does not result in fully homogenized liquid but simply lets the liquid to reach a different stage of solute segregation and clustering. Our results suggest that when cooling starts from a more viscous molten liquid ($T_q = 693$ K), precipitation of Phase X is difficult

(**Fig. 1d**); but when cooling starts from a less viscous molten liquid ($T_q = 723$ K), precipitation of Phase X is easier. Thus, the abnormal T_q -dependence of precipitation is connected to the molten liquid's structure at T_q .

One possible explanation of the observed precipitates could be the formation of high-temperature oxides. ³⁷ The Phase X formation is reproducible in hundreds of heating/cooling cycles of one sample, and the highest T is far below of oxides $T_{\rm m}$. The precipitation must have a different origin which is explored by isothermal analysis in the following paragraph.

Figure 2a presents an isothermal annealing protocol: i) the MG was heated up to 723 K at 2,000 K s⁻¹; ii) equilibrated by an isothermal hold for 0.1 s; iii) cooled down to annealing temperature of $T_A = 613-693 \text{ K}$ at 10,000 K s⁻¹; and iv) isothermally annealed for 0.5 s at a given T_A. If needed, the glass can immediately be re-heated after annealing to study any associated changes. During isothermal annealing, an exothermic peak was observed between ~0.01–0.04 s at $T_A \le 678$ K and was undetected when $T_A \ge 678$ K (Fig. 2b). In the subsequent re-heating, an endothermic peak, with an onset temperature of about 693±8 K, was always detected for the samples held at $T_A < 678$ K and not when $T_A \ge 678$ K (Fig. 2c). The exothermic peak on isothermal annealing and the endothermic peak on heating are reversible, of the same origin and connected with the Phase X formation as shown in Fig. 1b & d. Because 678 K is higher than $T_{\rm m}$, the presence of the exothermic peak during the isothermal annealing at $T_A < 678$ K implies that Phase X represents high-temperature precipitation that occurs above the eutectic temperature; because Phase X is only removed when the glass is heated above 693±8 K (see Supplemental Material Fig. S2). 38 Therefore, Phase X is a high- $T_{\rm m}$ precipitate, which is further confirmed by a time-temperature-transformation (TTT) diagram in Fig. 2d: Phase X is formed when $T > T_{\rm m}$, a critical $T_{\rm A} = 676$ K represents a critical supercooling $\Delta T = 74$ K, taken from T_1 , required for the Phase X formation. The TTT diagram also contains data of the 693 K-cooled glass for which T_q is set at 693 K (Fig. 2a). Again, the observations about the Phase X formation are the same. The incubation time of Phase X near $T_{\rm m}$ is ~0.012 s longer for the 693 K-cooled than for the 723 K-cooled glass suggesting a similar T_q -dependence of the precipitation as that resolved on continuous cooling (**Fig. 1d**).

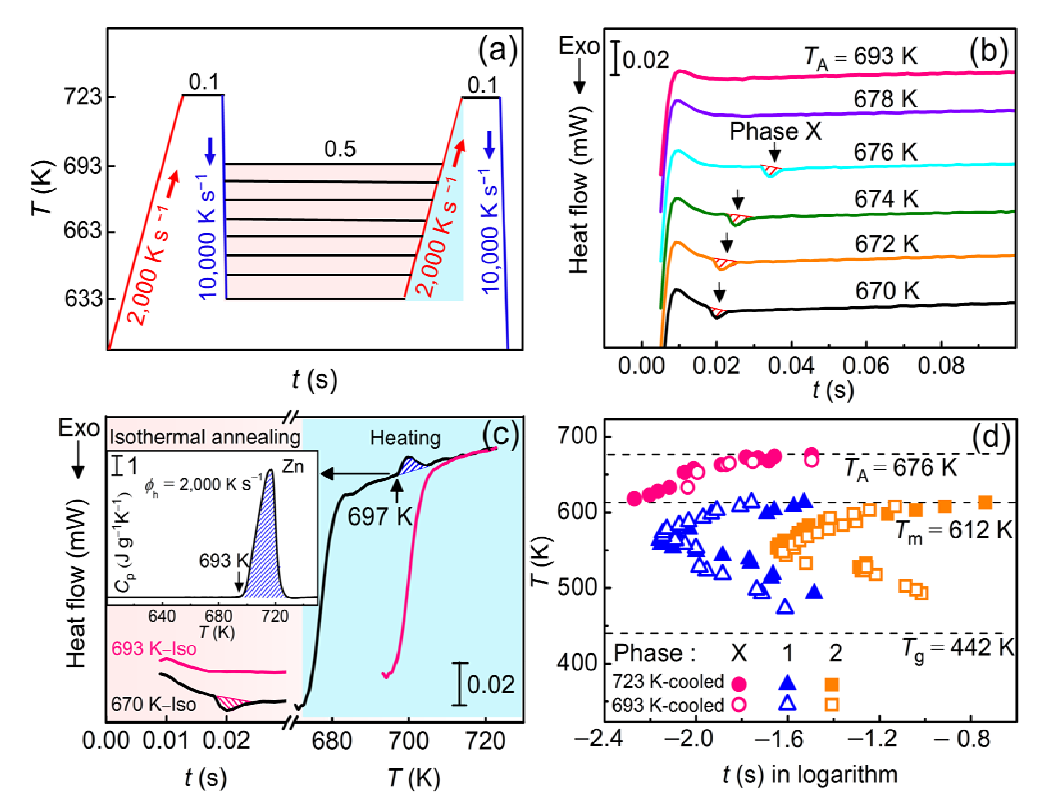


FIG. 2. (a) A thermal protocol of FDSC isothermal annealing of the off-eutectic Yb₄₇Mg₃₁Zn₁₉Cu₃ metallic glass (MG). (b) A small exothermic peak corresponding to phase X is detected during annealing between 670 and 676 K, and undetected for annealing temperature $T_A \ge 678$ K; all T_A lie above the melting temperature ($T_m = 612$ K) of the MG. Offset to the FDSC traces is applied for clarity. (c) The 670 K-annealed glass shows an exothermic peak (colored in red) at 0.018 s on isothermal annealing (left part) and an endothermic peak (colored in blue) starting at 697 K on the subsequent re-heating (right part). The 693 K-annealed glass shows neither an exotherm on annealing (left part) nor an endotherm on heating (right part) suggesting that the endothermic peak is a reversible process of the exothermic peak. Inset: Melting of pure Z_n in FDSC at $\phi_n = 2,000$ K s⁻¹ giving $T_m = 693$ K. (d) A time-temperature-transformation (TTT) diagram reveals the existence of three phases: Phase X (pink circles), Phase 1 (blue triangles) and Phase 2 (orange squares). The full and open symbols refer to the 723 K- and 693 K-cooled MGs, respectively. T_g is the glass-transition temperature.

In a search for the constituent elements to be the possible origin of the precipitation, Zn has $T_{\rm m}=693~{\rm K.}^{39}$ Pure Zn (99.99% purity, Jia-Ming-Bo-Ye Company) was re-measured by FDSC giving $T_{\rm m}=693\pm2$ at $\phi_{\rm h}=2,000~{\rm K~s^{-1}}$ (inset in **Fig. 2c**), lying in the temperature range of Phase X melting. Assuming that Phase X is a Zn precipitate, then its amount can be estimated to be $\approx0.1~{\rm ng}$ by taking the precipitation endothermic peak enthalpy of $\sim10~{\rm nJ}$; the Zn heat of fusion is 108 J g⁻¹. ³⁹ The precipitate mass represents $\sim0.3~{\rm wt.\%}$ of the total Zn content and $\sim0.04~{\rm wt.\%}$ of the MG, and we refer to them as Zn-rich precipitates. Neither high-energy X-ray diffraction (see Supplemental Material **Fig. S3**)³⁸ nor high-resolution transmission electron microscopy (see Supplemental Material **Fig. S4**)³⁸ can detect such a low amount of precipitates. Although we cannot provide direct experimental evidence for the presence of the Zn-rich precipitates, the above-given calorimetric results provide unambiguous indirect evidence.

Bearing the precipitation in mind, a new up-quenching strategy to make some off-eutectic MG compositions glassy is proposed. Yb₄₇Mg₃₁Zn₁₉Cu₃ represents an off-eutectic composition, and its T_1 is by 138 K higher than T_m (Fig. 1a). For this off-eutectic composition, the glass can only be made when quenched from $T_A < 693$ K (below T_I) at $\phi_c = 10,000$ K s⁻¹ because the precipitates — crystal nuclei — are mostly removed. This then gives a new thermal protocol (Fig. 3a). For a conventional "as-quenching" protocol, an MG is fully homogenized at $T > T_1$ and then directly quenched down to room temperature. For Yb₄₇Mg₃₁Zn₁₉Cu₃, by using such a conventional protocol, precipitation occurs at $\phi_c = 10{,}000$ K s⁻¹ resulting in solidification. A new "up-quenching" thermal protocol was introduced. The added "heating-up" step will melt precipitates while keeping the molten liquid below T_1 . The end temperature of the "heating-up" is above $T_{\rm m}$ of the precipitates, removing the supercooling condition as indicated by the dashed arrow in Fig. 3a. The molten liquid is homogenized at 693 K giving glass on consequent cooling. In the literature, ^{33,} ⁴⁰ up-quenching thermal protocol refers to a heating process at which heating is so rapid that no structural changes can occur before melting of the previously frozen phase, ⁴⁰ or to annealing of an alloy at temperatures slightly above the martensitic transformation temperature which is then quenched. ⁴¹ Here, the difference in terminology is to melt precipitate(s) during a heating process while keeping the molten liquid below T_1 . **Figure 3b** presents a proof-of-concept of the new strategy. In the as-quenching protocol, Yb₄₇Mg₃₁Zn₁₉Cu₃ was directly cooled from 763 K down to room temperature at $\phi_c = 10,000 \text{ K s}^{-1}$; at that condition the exothermic peak of solidification was unavoidable. By implementing the up-quenching protocol, the alloy was cooled from 763 K down to 613 K at $\phi_c = 10,000 \text{ K s}^{-1}$, then re-heated up to 693 K, and lastly quenched down to room temperature. In that case, neither precipitation nor crystallization peaks were observed demonstrating that the alloy is fully glassy and hence the new strategy is valid. Clearly, the fully glassy state can be reached when ϕ_c is higher than 10,000 K s⁻¹, as in the case of the melt-spinning and thin-film deposition, but when lower ϕ_c is required, as for the formation of BMG, an up-quenching protocol may be useful. Although this strategy has only been tested in Yb₄₇Mg₃₁Zn₁₉Cu₃ MG, it clearly may be valid for many other off-eutectic MG compositions with the equivalent liquid stability at $T < T_1$.

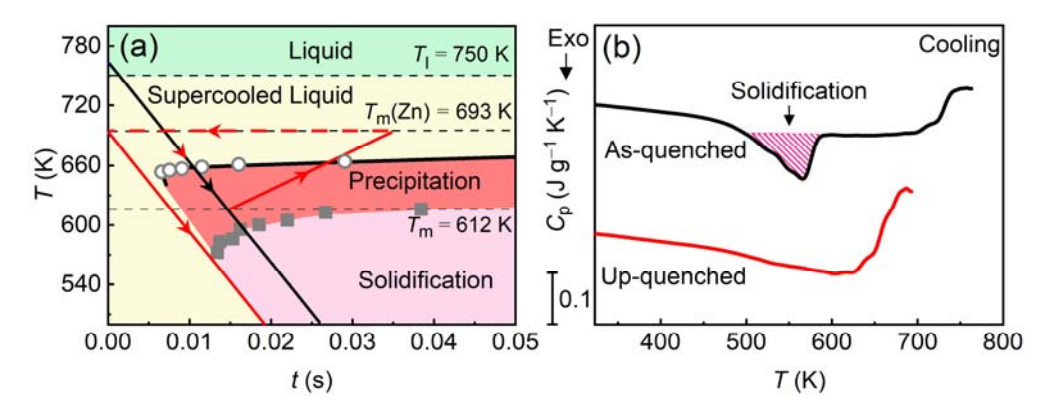


FIG. 3. (a) A schematic showing the application of an up-quenching thermal protocol (red arrows) to make the off-eutectic Yb₄₇Mg₃₁Zn₁₉Cu₃ glassy, which cannot be achieved by simple high-temperature melt-quenching (black arrow) giving crystalline alloy. An additional heating step is added to a conventional quenching protocol to melt any existing precipitates. (b) Fast DSC cooling traces of the as-quenched (black line) and the up-quenched (red line) alloys. The up-quenched glass was previously cooled from 763 K down to 613 K, then re-heated up to 693 K at $\phi_h = 4,000 \text{ K s}^{-1}$ and quenched at a cooling rate of 10,000 K s⁻¹ down to room temperature. The exothermic peak of solidification (red area) was observed for the as-quenched sample, only.

The present work demonstrates a novel phenomenon that an MG can be made at $T < T_1$ (**Fig. 1a & 1b**) when chemical diffusion or solute segregation are possible and phase separation like precipitation is suppressed. In this regard, the structural origin of this off-eutectic MG is a heterogenous solution instead of a homogeneous liquid. Although phase separation giving precipitation may occur in principle when the temperature is further decreased, the stability of the solution at $\phi_c = 10,000 \text{ K s}^{-1}$ in terms of the suppression of precipitation is good enough to allow the glass formation. According to the solubility-extension theory, 9 a precipitation onset temperature should decrease on fast cooling, which would be 663 K at 10, 000 K s⁻¹ for this MG (**Fig. 1b**). However, our results show that the precipitation temperature is not only ϕ_c dependent but also related to T_q . By lowering T_q to T_m of the precipitates, the glass can also be made below T_0 at the same ϕ_c . The GFA of this off-eutectic MG stems from the structural stability of its solution against phase separation but not solute segregation.

In summary, precipitation is identified by FDSC in a glass-forming metallic melt of Yb₄₇Mg₃₁Zn₁₉Cu₃. On cooling, starting from lower quenching temperature suppresses precipitation and improves the glass-forming ability. Higher quenching temperature deteriorates the glass formation due to the precipitation of a Zn-rich solid solution, which also occurs during isothermal annealing between the eutectic melting and liquidus temperature. The present work provides a new strategy to make some off-eutectic compositions containing elements that are not commonly used in glass formers glassy and may shed a light on a new origin of metallic glass: a solution instead of a liquid.

The authors thank Si Lan and Xun-Li Wang for their assistance with synchrotron X-ray scattering. This research used resources of the Advanced Photon Source, a U.S. Department of Energy (DOE) Office of Science User Facility operated for the DOE Office of Science by Argonne National Laboratory under Contract No. DE-AC02-06CH11357. This research was supported by the National Key Research and Development Plan (2018YFA0703603), the Strategic Priority Research Program of the Chinese Academy of Sciences (XDB30000000), the National Natural Science Foundation of China (11790291, 61999102, 61888102 and

51971239) and the Natural Science Foundation of Guangdong Province (2019B030302010), and JO and YHS acknowledge the financial support from the Center for International Collaboration, Institute of Physics. JO acknowledges the assistance provided by the Research Infrastructure NanoEnviCz, which is supported by the Ministry of Education, Youth and Sports of the Czech Republic (LM2015073). The authors declare that the data supporting the findings of this study are available within the paper and its supplementary information files. Correspondence and requests for materials should be addressed to JO (jiri.orava@ujep.cz) and YHS (ysun58@iphy.ac.cn).

REFERENCES

^{1.} W. Klement, R. H. Willens, and P. Duwez, Nature. **187**, 869 (1960).

² M. H. Cohen and D. Turnbull, Nature. **189**, 131 (1961).

^{3.} D. Wang, H. Tan, and Y. Li, Acta Mater. **53**, 2969 (2005).

⁴ Y. Wang, O. Wang, J. Zhao, and C. Dong, Scripta Mater. **63**, 178 (2010).

⁵ D. Wang, Y. Li, B. B. Sun, M. L. Sui, K. Lu, and E. Ma, Appl. Phys. Lett. **84**, 4029 (2004).

⁶ D. Turnbull, Contemp. Phys. **10**, 473 (1969).

⁷ Z. P. Lu, H. Tan, Y. Li, and S. C. Ng, Scripta Mater. **42**, 667 (2000).

^{8.} T. Egami and Y. Waseda, Journal of Non-Crystalline Solids. 64, 113 (1984).

^{9.} T. Egami and W. Johnson, in *Elements of Rapid Solidification*, edited by M.A. Otooni, (Springer-Verlag, Berlin, 1998), Chap. 1.

^{10.} Z. P. Lu and C. T. Liu, Acta Mater. **50**, 3501 (2002).

^{11.} J. Orava and A. L. Greer, J. Chem. Phys. **140**, 214504 (2014).

^{12.} H. Tan, Y. Zhang, D. Ma, Y. P. Feng, and Y. Li, Acta Mater. **51**, 4551 (2003).

^{13.} H. Ma, L. L. Shi, J. Xu, Y. Li, and E. Ma, Appl. Phys. Lett. **87**, 181915 (2005).

^{14.} W. H. Wang, J. J. Lewandowski, and A. L. Greer, J. Mater. Res. **20**, 2307 (2005).

^{15.} L. Xia, W. H. Li, S. S. Fang, B. C. Wei, and Y. D. Dong, J. Appl. Phys. **99**, 026103 (2006).

^{16.} K. F. Shamlaye, K. J. Laws, and J. F. Löffler, Acta Mater. **128**, 188 (2017).

^{17.} R. J. Highmore and A. L. Greer, Nature. **339**, 363 (1989).

- ^{18.} J. J. Z. Li, W. K. Rhim, C. P. Kim, K. Samwer, and W. L. Johnson, Acta Mater. **59**, 2166 (2011).
- ^{19.} C. Way, P. Wadhwa, and R. Busch, Acta Mater. **55**, 2977 (2007).
- ^{20.} M. E. Blodgett, T. Egami, Z. Nussinov, and K. F. Kelton, Sci. Rep. **5**, 13837 (2015).
- ^{21.} S. Wei, F. Yang, J. Bednarcik, I. Kaban, O. Shuleshova, A. Meyer, and R. Busch, Nat. Commun. 4, 2083 (2013).
- ^{22.} I. Jonas, F. Yang, and A. Meyer, Phys. Rev. Lett. 123 (2019).
- ^{23.} S. Küchemann and K. Samwer, Acta Mater. **104**, 119 (2016).
- ^{24.} W. Xu, M. T. Sandor, Y. Yu, H. B. Ke, H. P. Zhang, M. Z. Li, W. H. Wang, L. Liu, and Y. Wu, Nat. Commun. 6, 7696 (2015).
- ^{25.} C. Zhou, L. Hu, Q. Sun, J. Qin, X. Bian, and Y. Yue, Appl. Phys. Lett. **103**, 171904 (2013).
- ^{26.} X. Zhao, C. Wang, H. Zheng, Z. Tian, and L. Hu, Phys. Chem. Chem. Phys. 19, 15962 (2017).
- ^{27.} P. Zalden, F. Quirin, M. Schumacher, J. Siegel, S. Wei, A. Koc, M. Nicoul, M. Trigo, P. Andreasson, and H. Enquist, Science. 364, 1062 (2019).
- ^{28.} M. Stolpe, I. Jonas, S. Wei, Z. Evenson, W. Hembree, F. Yang, A. Meyer, and R. Busch, Phys. Rev. B. **93** (2016).
- ^{29.} R. Dai, R. Ashcraft, and K. F. Kelton, J. Chem. Phys. **148**, 204502 (2018)
- 30. C. Schick and V. Mathot, Fast Scanning Calorimetry, (Springer International Publishing, Switzerland, 2016).
- 31. Z. Lu, Y. Li, and S. Ng, Journal of Non-Crystalline Solids. 270, 103 (2000).
- ^{32.} S. Pogatscher, D. Leutenegger, J. E. K. Schawe, P. J. Uggowitzer and J. F. Löffler, Nat. Commun. 7, 11113 (2016).
- ^{33.} J. E. K. Schawe and J.F. Löffler, Nat. Commun. **10**, 1337 (2019).
- ^{34.} W. Kurz and D. J. Fisher, Fundamentals of Solidification, (Enfield Publishing & Distribution Company, USA, 1992).
- 35. W.J. Boettinger, U. R. Kattner, K.-W. Moon and J. H. Perepezko, in Methods for Phase Diagram Determination, edited by J.-C. Zhao, (Elsevier Ltd. Netherlands, 2007), Chap. 5.
- ^{36.} M. Bugnet, A. Kula, M. Niewczas, and G. A. Botton, Acta Mater. **79**, 66 (2014).

- ^{37.} H. Lin, W. L. Johnson, and W. K. Rhim, Materials Transactions, JIM **38**, 473 (1997).
- ^{38.} See Supplemental Materials at [URL] for Figs. S2, S3 and S4.
- ^{39.} W. M. Haynes, CRC Handbook of Chemistry and Physics, (CRC Press, USA, 2014).
- ^{40.} G. Kurtuldu, K.F. Shamlaye, and J.F. Löffler, Proc. Natl. Acad. Sci. U. S. A. 115, 24 (2018).
- ^{41.} S.S. Leu and C.T. Hu, Up-quenching effect on the stabilization process of a Cu-Zn-Al martensite. Mater. Sci. Eng. A **177**, 247 (1989).